24th COBEM - 2017

24th ABCM International Congress of Mechanical Engineering
December 3-8, 2017, Curitiba, PR, Brazil

COBEM-2017-0272
KINEMATIC MODELING OF 5R PARALLEL SYMMETRICAL MECHANISM SUBJECTED TO UNCERTAINTIES

Fabian Andres Lara-Molina
Tyago Fylipe Vieira Proenca
Leandro Augusto Martins
Departament of Mechanical Engineering, Federal University of Technology - Paraná, Cornélio Procópio- PR, CEP 86300-000, Brazil
fabianmolina@utfpr.edu.br, leandromartins@alunos.utfpr.edu.br

Abstract. *This paper aims at analyzing the kinematic model of the 5R parallel symmetrical mechanism subject to uncertainties. The kinematic model describes the forward kinematics, the workspace and the kinematic dexterity represented by the Global Conditioning Index (GCI). The uncertainties are modeled as random variables and these uncertainties are introduced in the dimensions of links and also in the clearances of the active joints. Additionally, the sensitivity analysis permits to evaluate the influence of each uncertain parameter on the model. Simulation results permit evaluating the forward kinematics, workspace, and GCI with uncertainties.*

Keywords: *Kinematic, Uncertainties, Global Conditioning Index, Sensitivity Analysis*

1. INTRODUCTION

The mechanisms are unavoidably subject to uncertainties. The main sources of uncertainties include various issues such as manufacturing limitations and assembling tolerances of the mechanical parts. Despite these uncertainties and specifically, the parallel mechanism should be able to operate with high accuracy and repeatability which requires high reliability, e.g. the mechanism applied in robots used in medical applications. Consequently, it is necessary to analyze the effects of these uncertainties on the kinematics in order to evaluate the behavior of the parallel mechanism under these conditions.

The stochastic approach has been widely applied in order to analyze the effects of uncertain parameters on the behavior of the robot mechanism. In agreement with this approach, the effect of tolerances associated with the manipulator parameters on the reliability was studied by (Kim et al., 2010; Lara-Molina et al., 2015). Moreover, the Polynomial Chaos Theory was applied to study the effect of uncertain inertia and payload on SCARA robot dynamics Voglewede et al. (2009). Additionally, an approach based on fuzzy dynamic analysis has been applied to study uncertain parameters in a robot manipulator Lara-Molina et al. (2014). The aforementioned approaches are suitable when the stochastic process that governs the uncertainty is completely characterized.

According to the previous discussion, it is necessary to analyze the kinematics of parallel mechanism under uncertain parameters, i.e., to analyze how the mechanism is affected by uncertainties, and thus to quantify these effects into the kinematics by using straightforward numerical methods based on the uncertainty analysis and the sensitivity analysis.

This paper aims at analyzing the kinematics of the 5R parallel mechanism subjected to an uncertain length of the links and clearances of the active joints. In accordance with that, the forward kinematic model and the workspace were formulated as a function of the aforementioned uncertain parameters. The uncertain parameters are modeled as random variables and they are introduced in the kinematic model of the mechanism. The Monte Carlo Simulation is the stochastic solver used in order to compute the numerical response of the kinematic model with the uncertain parameters. Moreover, the sensitivity analysis aims at determining the influence of each uncertain parameter on the kinematics of the mechanism, specifically in terms of the variation of the position accuracy of the mechanism. Finally, the numerical results are analyzed.

The remaining of paper is organized as follows. The section 2. introduces the kinematic model of the parallel mechanism. In the section 3, the stochastic uncertainty analysis and the sensitivity analysis are presented. The numerical results are shown in section 4. Finally, the conclusions and further work are outlined.

2. KINEMATIC MODEL

The 5R planar parallel mechanism has two active or actuated joints, three passive of free joints and four links. The geometry of the 5R symmetrical parallel mechanism is defined according to Fig. 1. The active joints are located at A_i and they are denoted as θ_i (for $i = 1,2$). The passive joints are located at the end of each link of the active joints B_i.

The end-effector of the mechanism is located at P that is defined by the x and y cartesian coordinates. Additionally, the fixed reference frame O is defined in the middle of A_1A_2, therefore the symmetry of the mechanism is defined by $OA_1 = OA_2$, $A_1B_1 = A_2B_2$ and $B_1P = B_2P$. Consequently, the geometry of the 5R symmetrical mechanism can be defined by $OA_i = \bar{r}_3(r_3)$, $A_iB_i = \bar{r}_1(r_1)$ and $B_iP = \bar{r}_2(r_2)$.

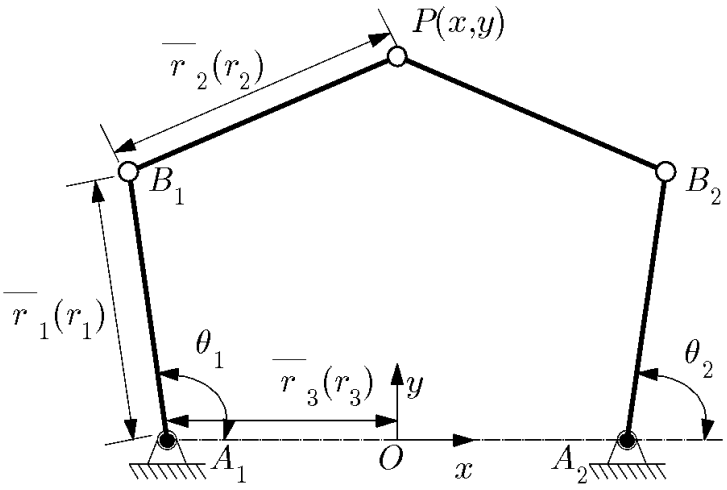

Figure 1. The 5R symmetrical parallel mechanism

2.1 Inverse Kinematics

The inverse kinematic model permits to define the active joints θ_i as a function of the position of end-effector P. The position, P, of the end-effector with respect of the fixed reference frame O is defined by the Cartesian vector $\mathbf{p} = \begin{bmatrix} x & y \end{bmatrix}^T$. Additionally, the position of the points B_i (for $i = 1,2$) with respect to the fixed frame O is defined by the vector $\mathbf{b}_1 = \begin{bmatrix} r_1\cos(\theta_1) - r_3 & r_1\sin(\theta_1) \end{bmatrix}^T$ and $\mathbf{b}_2 = \begin{bmatrix} r_1\cos(\theta_2) + r_3 & r_1\sin(\theta_2) \end{bmatrix}^T$, respectively. The inverse kinematics is solved with the aids of the constraint equation $|\mathbf{b}_i\mathbf{p}| = r_2$, therefore:

$$(x - r_1\cos(\theta_1) - r_3)^2 + (y - r_1\sin(\theta_1))^2 = r_2^2 \tag{1}$$
$$(x - r_1\cos(\theta_2) + r_3)^2 + (y - r_1\sin(\theta_2))^2 = r_2^2 \tag{2}$$

by solving Eqs. (1) and (2) with $\mathbf{p}$ being known, θ_i can be determined by using the following expressions:

$$\theta_i = 2\tan^{-1}(z_i) \tag{3}$$

where

$$z_i = \frac{-b_i + \sigma_i\sqrt{b_i^2 - 4a_ic_i}}{2a_i} \tag{4}$$

with
$\sigma_i = \pm 1$
$a_1 = r_1^2 + y^2 + (x + r_3)^2 - r_2^2 + 2(x + r_3)r_1$
$b_1 = -4yr_1$
$c_1 = r_1^2 + y^2 + (x + r_3)^2 - r_2^2 - 2(x + r_3)r1$
$a_2 = r_1^2 + y^2 + (x - r_3)^2 - r_2^2 + 2(x - r_3)r_1$
$b_2 = b_1 = -4yr_1$
$c_2 = r_1^2 + y^2 + (x - r_3)^2 - r_2^2 - 2(x - r_3)r1$

As seen in Eq. (4), the inverse kinematic has four different solutions that depend on the signal adopted by σ_i. The solution adopted in this paper considers $\sigma_1 = 1$ and $\sigma_2 = -1$. Based on Eqs. (3) and (4), the inverse kinematic can be expressed by the fallowing expression:

$$\begin{bmatrix} \theta_1 & \theta_2 \end{bmatrix}^T = f(x, y, r_1, r_2, r_3) \tag{5}$$

2.2 Forward Kinematics

The forward kinematic model sets the position of end effector P as function of the active joints θ_i. The forward kinematics is obtained from Eqs. (1) and (2):

$$x^2+y^2-2(r_1\cos(\theta_1)-r_3)x-2r_1\sin(\theta_1)y-2r_1r_3\cos(\theta_1)+r_3^2+r_1^2-r_2^2=0 \tag{6}$$
$$x^2+y^2-2(r_1\cos(\theta_2)+r_3)x-2r_1\sin(\theta_2)y+2r_1r_3\cos(\theta_2)+r_3^2+r_1^2-r_2^2=0 \tag{7}$$

By using the Eqs. (6) and (7) are derived the following expressions:

$$x=ey+f \tag{8}$$

with $e=\frac{r_1(\cos(\theta_1)-\sin(\theta_1))}{2r_3+r_1\cos(\theta_2)-r_1\cos(\theta_1)}$ and $f=\frac{r_1r_3(\cos(\theta_1)+\cos(\theta_2))}{2r_3+r_1\cos(\theta_2)-r_1\cos(\theta_1)}$. By substituting Eq. (8) to Eq. (6), it is obtained:

$$dy^2+gy+h=0 \tag{9}$$

with
$d=1+e^2$
$g=2(ef-er_1\cos(\theta_1)+er_3-r_1\sin(\theta_1))$
$h=f^2-2f(r_1\cos(\theta_1)-r_3)-2r_1r_3\cos(\theta_1)+r_3^2+r_1^2-r_2^2$
Considering Eq. (9), y can be obtained:

$$y=\frac{-g+\sigma\sqrt{g^2-4dh}}{2d} \tag{10}$$

From Eq. (10) is observed that the forward kinematic has two solutions corresponding to $\sigma=1$ or $\sigma=-1$. Based on Eqs. (8) and (10), the forward kinematic formulation can be summarized by the fallow expression:

$$\begin{bmatrix}x & y\end{bmatrix}^T=f^{-1}(\theta_1,\theta_2,r_1,r_2,r_3) \tag{11}$$

2.3 Jacobian Matrix

In order to derive the Jacobian matrix of the mechanism Eqs. (1) and (2) are differentiated with respect to time to obtain:

$$r_1(y\cos(\theta_1)-(x+r_3)\sin(\theta_1))\dot{\theta}_1=(x+r_3-r_1\cos(\theta_1))\dot{x}+(y-r_1\sin(\theta_1))\dot{y} \tag{12}$$
$$r_1(y\cos(\theta_2)+(r_3-x)\sin(\theta_2))\dot{\theta}_2=(x-r_3-r_1\cos(\theta_2))\dot{x}+(y-r_1\sin(\theta_2))\dot{y} \tag{13}$$

the Eqs. (12) and (13) are written in the matricial form:

$$\mathbf{A}\dot{\theta}=\mathbf{B}\dot{\mathbf{p}} \tag{14}$$

where $\dot{\mathbf{p}}=\begin{bmatrix}\dot{x} & \dot{y}\end{bmatrix}^T$, $\dot{\theta}=\begin{bmatrix}\dot{\theta}_1 & \dot{\theta}_2\end{bmatrix}^T$ and the 2×2 matrices $\mathbf{A}$ and $\mathbf{B}$:
$\mathbf{A}=\begin{bmatrix}y\cos(\theta_1)-(x+r_3)\sin(\theta_1) & 0\\ 0 & y\cos(\theta_2)+(r_3-x)\sin(\theta_2)\end{bmatrix}$
$\mathbf{B}=\begin{bmatrix}x+r_3-r_1\cos(\theta_1) & y-r_1\sin(\theta_1)\\ x-r_3-r_1\cos(\theta_2) & y-r_1\sin(\theta_2)\end{bmatrix}$
The Jacobian matrix is expressed as:

$$\mathbf{J}=\mathbf{A}^{-1}\mathbf{B} \tag{15}$$

2.4 Maximum Inscribed Workspace

The Maximum Inscribed Circle (MIC) is useful to evaluate the flatness of the usable workspace, the MIC is inscribed within the usable workspace and it is tangent with singular loci Liu et al. (2006). The Maximum Inscribed Workspace (MIW) is defined as the workspace bounded by the MIC. The MIC is characterized by the expressions:

$$x^2+(y-y_{MIC})^2=r_{MIC}^2 \tag{16}$$

where r_{MIC} is the radius and $(0, y_{MIC})$ is the center. For the cases when $r_1 + r_3 < r_2$, the MIC is defined by

$$\begin{aligned} r_{MIC} &= (r_1 + r_2 - |r_1 - r_2|)/2 \qquad \text{and} \\ y_{MIC} &= \sqrt{(r_1 + r_2 + |r_1 - r_2|)^2/4 - r_3^2} \end{aligned} \tag{17}$$

For the cases when $r_1 + r_3 > r_2$, the radius and center of the MIC are defined by:

$$\begin{aligned} r_{MIC} &= |y_{MIC}| - y_{col} \qquad \text{and} \\ y_{MIC} &= \frac{(r_1 + r_2 + y_{col})^2 - r_3^2}{2(r_1 + r_2 + y_{col})} \end{aligned} \tag{18}$$

with $y_{col} = \sqrt{r_1^2 - (r_2 - r_3)^r}$. Based of Eqs. (16), (17) and (18), the MIW can be expressed by using the follow expression:

$$\begin{bmatrix} r_{MIW} & y_{MIW} \end{bmatrix} = g(r_1, r_2, r_3) \tag{19}$$

where g is the the mathematical expression that computes r_{MIW} and y_{MIW} based on r_1, r_2 and r_3. Figure 2 shows the workspace for two different sets of link lengts, in Fig. 2(a) r_1=1.2, r_2=1 and r_3=0.8 and in Fig. 2(a) r_1=1, r_2=1.2 and r_3=0.8.

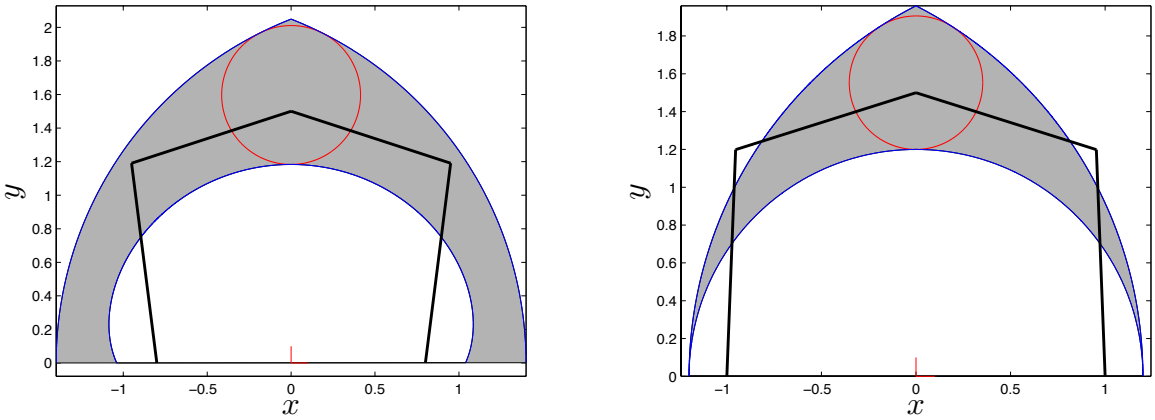

(a) (b)

Figure 2. Maximum Inscribed Workspace

2.5 Global Conditioning Index

The kinematic dexterity is an important property that is considered in the optimal design of parallel mechanism. The dexterity is the skill to handle an object with accuracy, this kinematic characteristic of the manipulator is measured in terms of the Jacobian matrix due to its physical meaning. The Jacobian matrix of Eq. (15) can be factored by using the singular value decomposition:

$$\mathbf{J} = [\mathbf{U}^T][\Sigma][\mathbf{V}] \tag{20}$$

in which Σ is a diagonal composed of the singular values. Therefore, we have two singular values $\sigma_1 > \sigma_2 > 0$. The condition number is $k(\mathbf{J}) = \sigma_1/\sigma_2$.

A commonly used criterion to evaluate the dexterity is the global conditioning index (GCI) Angeles and Gosselin (1991). The reciprocal of the condition number is used as the measure of the local kinematic dexterity, thus $1/k(\mathbf{J})$ varies from 0 (singular condition) to 1 (isotropic condition). For a defined workspace w, the GCI is defined as:

$$GCI = \frac{\int_w 1/k(\mathbf{J}) dw}{\int_w dw} \tag{21}$$

Specifically, for this contribution the MIW is considered as the workspace over the GCI is computed, thus, $w = MIW$. The greater the global conditioning index indicates more dexterity over the workspace, therefore the global conditioning index should be maximized in the optimal design procedure.

3. STOCHASTIC ANALYSIS

Typically the geometrical parameters of the parallel mechanism are affected by uncertainties. Manufacturing tolerances include small variations in the geometrical parameters (Paccot et al., 2009; Lara-Molina et al., 2014). Therefore, the parameters selected in order to introduce the uncertainties in the model presented in the previous section are: the length of the non-dimensional links (r_1, r_2 and r_3), and additionally in the active joints θ_1 and θ_2.

3.1 Uncertain Parameter Model

The uncertain parameters are modeled as random variables. The corresponding uncertainties are introduced by using the relation:

$$a_0(\Theta) = a_0 + a_0\delta_a\xi(\Theta) \tag{22}$$

where a_0 is the mean value of the parameter, δ_a is the dispersion level and $\xi(\Theta)$ is the unite normal random variable with Θ being a random process. The unit normal random variable is governed by a normal distribution, this distribution was selected in order to evaluate the uncertain parameters in this contribution.

The so-called Monte Carlo method combined with the Latin Hypercube sampling Florian (1992) is used to simulate the dynamic response of the robot with the considered uncertain random parameters. Additionally, with the aid of a convergence analysis is determinated the number of Monte Carlo samples n_s to obtain an accurate result in the simulations.

3.2 Sensitivity Analysis

The previous sections presented the mechanism modeling. The sensitivity analysis aims at determining the influence of each uncertain parameter on the kinematics of the mechanism, specifically in terms of the variation of the position accuracy of the mechanism. Consequently, this analysis allows indicating the degree of influence of each uncertain parameter on the variation of the position accuracy of the mechanism.

Among the various methods used to analyze the sensitivity, the variance-based sensitivity analysis decomposes the variance of the output of the model into fractions which are associated with the variation of each parameter Saltelli et al. (2008). This method allows quantifying the effect of the variation of an individual parameter on the kinematic response by means of a probabilistic framework based on the Monte Carlo Simulation method. Additionally, this method copes with nonlinear models, which is suitable to quantify the sensitivity of the parallel mechanism.

Considering the model under the form $y = f(\mathbf{w})$, where y is a scalar output and $\mathbf{w} = \begin{bmatrix} w_1 & \dots & w_k \end{bmatrix}^T \in \mathbb{R}^{k\times 1}$ is a vector of k parameters. These parameters are considered as independently and uniformly distributed within the unit hypercube, i.e., $w_i \in [0,1]$ for $i = 1,\dots,k$. $f(\mathbf{w})$ is decomposed:

$$y = f(\mathbf{w}) = f_0 + \sum_{i=1}^{k} f_i(w_i) + \sum_{i<j}^{k} f_{ij}(w_i,w_j) + \cdots + f_{12\dots,k} \tag{23}$$

The decomposition of the variance expression is (Sobol', 1990):

$$V(y) = \sum_{i=1}^{k} V_i + \sum_{i<j}^{k} V_{ij} + \cdots + V_{12\dots k} \tag{24}$$

where $V_i = V_{w_i}(E_{\mathbf{w}_{\sim i}}(y|w_i))$, $V_{ij} = V_{w_{ij}}(E_{\mathbf{w}_{\sim ij}}(y|w_{ij}))$, and so on. A variance based first order effect for a generic design parameter w_i is:

$$V_{w_i}(E_{\mathbf{w}_{\sim i}}(y|w_i)) \tag{25}$$

where w_i is the i-th parameter and $\mathbf{w}_{\sim i}$ denotes the matrix of all parameters except w_i. The meaning of the inner expectation operation is that the mean of y is taken over all possible values $\mathbf{w}_{\sim i}$ while keeping w_i fixed. The associated sensitivity measure denominated first-order sensitivity index is defined as:

$$s_i = \frac{V_{w_i}(E_{\mathbf{w}_{\sim i}}(y|w_i))}{V(y)} \tag{26}$$

s_i states the effect of the variation of w_i only, however divided by the variation in other parameters. Nevertheless, the total effect-index s_{Ti} measures the contribution to the output variance of w_i, including all the effects of its interactions with any other input parameter.

$$s_{Ti} = \frac{E_{\mathbf{w}_{\sim i}}(V_{w_i}(y|w_{\sim i}))}{V(y)} = 1 - \frac{V_{\mathbf{w}_{\sim i}}(E_{w_i}(y|w_{\sim i}))}{V(y)} \tag{27}$$

The Monte Carlo Simulation combined with the Latin Hypercube sampling Florian (1992) is used to calculate the total-effect indices. The total number of model evaluation to compute the total-sensitivity index is $N = n_s(k+1)$, where n_s is the number of the Monte Carlo samples (Saltelli et al., 2008).

4. SIMULATION RESULTS

The uncertain parameters of the parallel mechanism for the inverse, forward kinematics and workspace are considered as random variables. These random variables are defined based on the Eq. (22). The parameters of the non-dimensional length of the links (r_1, r_2 and r_3) and the clearances of the active joints ($\delta\theta_1$, $\delta\theta_2$) are defined in Table 1. Therefore, the active joints are defined with the uncertainties as $\theta_i(\Theta) = \theta_i + \delta\theta_i(\Theta)$.

Table 1. Uncertain Parameters of the manipulator

Parameter	$r_1(\Theta)$	$r_2(\Theta)$	$r_3(\Theta)$	$\delta\theta_1(\Theta)$	$\delta\theta_2(\Theta)$
a_0	1.2	1.0	0.8	0.25^o	0.25^o
δ_a	1%	1%	1%	100%	100%

The uncertain parameters of the mechanism are mapped on the kinematic model by using the Monte Carlo Simulation in order to evaluate the kinematics of mechanism in the presence of uncertainties. For this, n_s=150 samples are used to compute the Monte Carlo Simulation.

4.1 Forward Kinematics

This analysis aims at evaluating the forward kinematics of the mechanism considering uncertainties in the non-dimensional link lengths and the clearances of the active joints that were previously described in Table 1. Consequently, the uncertainties were introduced in the forward kinematic model based on Eq. (28).

$$\begin{aligned}&\begin{bmatrix} x(\Theta) & y(\Theta) \end{bmatrix}^T = \\ &f^{-1}(\theta_1 + \delta\theta_1(\Theta), \theta_2 + \delta\theta_2(\Theta), r_1(\Theta), r_2(\Theta), r_3(\Theta))\end{aligned} \tag{28}$$

The forward kinematic with the uncertain parameters of Eq. (28) was evaluated for several poses (θ_i) within the usable workspace as presented in Fig. 3. Additionally, Fig. 3 shows the usable workspace and the MIW for r_1=1.2, r_2=1.0 and r_3=0.8.

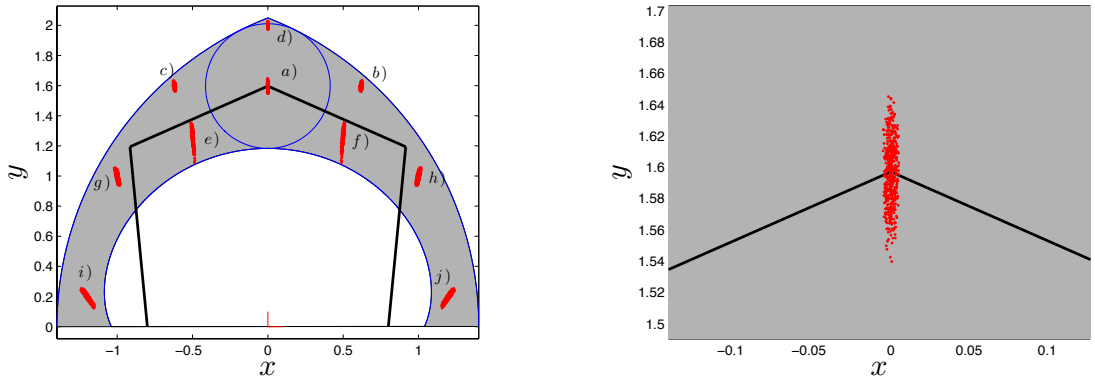

(a) (b)

Figure 3. Forward Kinematic solutions with uncertain parameters: (a) For all cases, (b) Zoom of case a)

Additionally, Table 2 presents the results of the forward kinematics which are mean and standard deviation the Cartesian position of the end effector in the x and y axis, $\bar{x}$, $\bar{y}$, σ_x, σ_y, respectively.

The results indicates that the uncertainties in the non-dimensional lengths of the links and the clearances of the active joints introduce a variability in the Cartesian position of the end effector of the mechanism, **p**, for all the cases considered in this analysis, this variability is quantified by the standard deviation σ_x and σ_y of each single pose. The variability in **p** is specially larger for the configurations closed to the singular loci singularities (cases: e), f), i) and j)). Additionally,

Table 2. Forward Kinematic with Uncertainties

Case	θ_1	θ_2	$\overline{x}$	$\overline{y}$	σ_x	σ_y
a)	95.51	84.48	3.5586e-08	1.5966	0.0020	0.0193
b)	60.88	58.03	0.6200	1.5969	0.0040	0.0138
c)	121.96	119.11	-0.6200	1.5969	0.0040	0.0139
d)	78.89	101.10	-6.3229e-07	2.0000	0.0013	0.0110
e)	123.53	104.77	-0.4996	1.2648	0.0046	0.0439
f)	75.22	56.46	0.4996	1.2648	0.0048	0.0439
g)	154.10	132.20	-0.9998	0.9990	0.0071	0.0247
h)	47.79	25.89	0.9998	0.9990	0.0072	0.0245
i)	27.47	-26.83	1.1988	0.1982	0.0179	0.0260
j)	-153.16	152.52	-1.1988	0.1982	0.0177	0.0259

it is observed that the poses closed to the limits of the usable workspace have a moderate variability with respect to the previous cases (cases: b), g) and h)). However, for the poses within the MIW, the forward kinematics exhibits a smaller variability (cases: a) e d)).

The sensitivity analysis was performed for the case a) of Table 2, however any other position could be considered. The total effect-indices of the uncertain parameters of table 1 are computed by using the variance-based sensitivity analysis presented in section 3.2

The total effect-indices for the forward kinematics are showed in Fig. 4. As seen, the position accuracy is more sensitive to length of the links. This is expected since the length of the links is proportional to the positioning of the end-effector of mechanism. However, among the uncertain parameters the clearances of active joints exhibit a significant sensitivity.

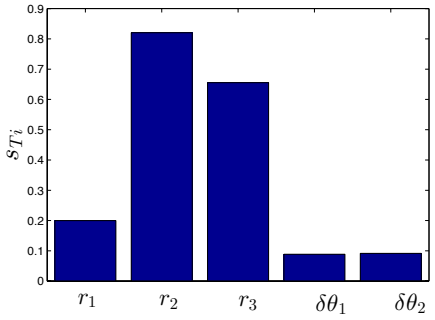

Figure 4. Sensitivity indices of the Forward with uncertainties

4.2 Workspace

The usable workspace and MIW are also determined as function of the uncertain non-dimensional lengths of the links $r_1(\Omega)$, $r_1(\Omega)$ and $r_1(\Omega)$ presented in Table. 1. Based on Eq. (19), the MIW with the uncertain parameters can be obtained by using the follow expression:

$$\begin{bmatrix} r_{MIW}(\Omega) & y_{MIW}(\Omega) \end{bmatrix} = g(r_1(\Omega), r_2(\Omega), r_3(\Omega)) \tag{29}$$

As presented in Fig. 5, the uncertainties in the non-dimensional lengths introduce an small variability in the shape of the usable workspace and the MIW.

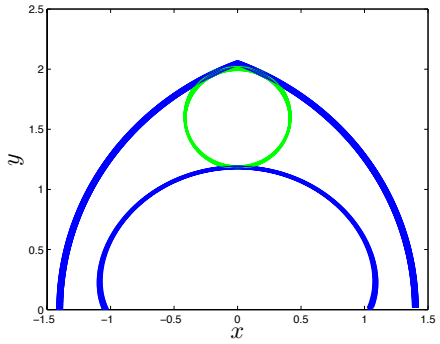

Figure 5. Usable and Maximum Inscribed Workspace with uncertanties

The variability of the MIW is presented in Table 3. It is also observed that the uncertain parameters introduce a variability in the center and radius of the MIC, this could produce also a variability in the kinematic performance of the 5R symmetric mechanism, specifically in the Global Condition Index that is evaluated over the MIW (Liu et al., 2006).

Table 3. Maximum Inscribed Workspace with Uncertainties

$\overline{r}_{MIW}$	$\overline{y}_{MIW}$	$\sigma_{r_{MIW}}$	$\sigma_{y_{MIW}}$
0.4138	1.5970	0.0041	0.0085

Moreover, the total effect-indices for the MIW are showed in Fig. 6. The MIW model was previously defined in Eq. (29) as function of the length of the links, specifically, the sensitivity of the radius of MIW r_{MIW} was evaluated. The total effect-indices indicate that r_2 is most sensitive parameter. However, r_3 also shows a remarkable sensitivity.

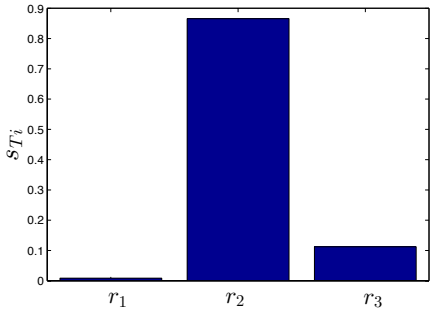

Figure 6. Sensitivity indices of the Workspace with uncertainties

4.3 Global Conditioning Index

The GCI is also determined as function of the uncertain non-dimensional lengths of the links $r_1(\Omega)$, $r_1(\Omega)$ and $r_1(\Omega)$ and the clearances of the active joints $\delta\theta_1(\Omega)$ and $\delta\theta_2(\Omega)$ presented in Table. 1. Based on Eq. (21), the GCI with the uncertain parameters can be obtained by using the follow expression:

$$GCI(\Omega) = f(r_1(\Omega), r_2(\Omega), r_3(\Omega), \delta\theta_1(\Omega), \delta\theta_2(\Omega)) \tag{30}$$

The total effect-indices for the GCI are showed in Fig. 7. For this specific set of the length of the links, the GCI is highly sensitive to the the length of the links. The clearances of the active joints show a considerable sensitivity taking into account the fact that these parameters introduce small position errors in the Jacobian that is used to compute GCI.

5. CONCLUSIONS

This paper presented a methodology to evaluate the kinematic model of the planar 5R parallel mechanism with uncertainties by using a stochastic analysis. The uncertain were considered in the non-dimensional link lengths and the

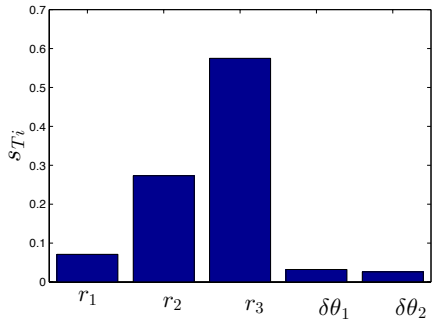

Figure 7. Sensitivity indices of the GCI with uncertainties

clearances of the active joints, these uncertain parameters were modeled as random variables. The forward kinematics, inverse kinematic and workspace were evaluated by using the Monte Carlo Simulation.

Moreover, the sensitivity analysis allowed determining the contribution of each uncertain parameter on the uncertain response of the mechanism. This is important to determine the degree of importance of the uncertain parameters on the kinematic of the mechanism.

Simulation results indicated a non-negligible variability in the kinematics of the mechanism produced by the uncertain parameters. Consequently, the effects produced by the uncertainties should be taken into account in order to design parallel mechanism subjected to uncertainties.

6. ACKNOWLEDGEMENTS

The authors express their acknowledgements to the Graduate Program in Mechanical Engineering of the Federal University of Technology - Paraná funded by CAPES.

7. REFERENCES

Kim, J.; Song, W.-J.; Kang, B.-S. *Applied Mathematical Modelling* **2010**, *34*, 1225–1237.

Lara-Molina, F.; Koroishi, E.; Dumur, D.; Jr., V. S. *IFAC-PapersOnLine* **2015**, *48*, 214 – 219, 11th {IFAC} Symposium on Robot Control {SYROCO} 2015Salvador, Brazil, 26âĂŞ28 August 2015.

Voglewede, P.; Smith, A. H. C.; Monti, A. *IEEE Transactions on Robotics* **2009**, *25*, 206–210.

Lara-Molina, F.; Koroishi, E.; Steffen, V. Uncertainty Analysis of a Two-Link Robot Manipulator under Fuzzy Parameters. Robotics: SBR-LARS Robotics Symposium and Robocontrol (SBR LARS Robocontrol), 2014 Joint Conference on. 2014; pp 1–6.

Liu, X.-J.; Wang, J.; Pritschow, G. *Mechanism and Machine Theory* **2006**, *41*, 119–144.

Angeles, J.; Gosselin, C. *Journal of Mechanical Design* **1991**, *113*, 220–226.

Paccot, F.; Andreff, N.; Martinet, P. *The International Journal of Robotics Research* **2009**, *28*, 395–416.

Lara-Molina, F. A.; Rosário, J. M.; Dumur, D.; Wenger, P. *Industrial Robot: An International Journal* **2014**, *41*, 275 – 285.

Florian, A. *Probabilistic engineering mechanics* **1992**, *7*, 123–130.

Saltelli, A.; Ratto, M.; Andres, T.; Campolongo, F.; Cariboni, J.; Gatelli, D.; Saisana, M.; Tarantola, S. *Global Sensitivity Analysis: The Primer*; John Wiley & Sons Chichester, England, 2008.

Sobol', I. M. *Matematicheskoe Modelirovanie* **1990**, *2*, 112–118.

Liu, X.-J.; J., W.; Pritschow, G. *Mechanism and Machine Theory* **2006**, *41*, 145–169.

8. RESPONSIBILITY NOTICE

The authors are the only responsible for the printed material included in this paper.